LA-UR-87-2105 (revised)

CONF-871142--1-Rev.

TITLE THE TAB METHOD FOR NUMERICAL CALCULATION OF SPRAY DROPLET BREAKUP

LA-UR--87-2105-Rev.

DE87 011756

AUTHOR(S) Peter J. O'Rourke and Anthony A. Amsden

SUBMITTED TO 1987 International Fuels and Lubricants Meeting and Exposition, Toronto Hilton Hotel, Toronto, Ontario, November 2-5, 1987

DISCLAIMER

Los Alamos Los Alamos National Laboratory
Los Alamos, New Mexico 87545

FORM NO 836 R4
ST NO 2629 5/81

MASTER

THE TAB METHOD FOR NUMERICAL CALCULATION OF SPRAY DROPLET BREAKUP

By

Peter J. O'Rourke and Anthony A. Amsden
Theoretical Division, Group T-3
Los Alamos National Laboratory
Los Alamos, New Mexico 87545

ABSTRACT

We present a method for calculating drop aerodynamic breakup in engine sprays. A short history is first given of the major milestones in the development of the stochastic particle method for calculating liquid fuel sprays. The most recent advance has been the discovery of the importance of drop breakup in engine sprays. We present a new method, called the TAB method, for calculating drop breakup. Some theoretical properties of the method are derived; its numerical implementation in the computer program KIVA is described; and comparisons are presented between TAB-method calculations and experiments and calculations using another breakup model.

INTRODUCTION AND BACKGROUND

Until recently, the detailed analysis of practical sprays was impossible due to the complexity of the physical processes occurring. The first step toward solving this problem was taken when a statistical formulation was proposed for spray analysis (1) for similar reasons that motivated most common approaches to turbulence modeling in single phase fluid flows. But even with this simplification, the mathematical problem was formidable and could be analyzed only when very restrictive assumptions were made. This is because the statistical formulation required the solution of the spray equation determining the evolution of the probability distribution function of droplet locations, sizes, velocities, and temperatures. The spray equation resembles the Boltzmann equation of gas dynamics (2) but has more independent variables and more complex terms on its right-hand side representing the effects of collisions, breakups, and nucleations.

Two numerical methods have been used for the solution of the spray equation. In the first (3,4), the full distribution function f is found approximately by subdividing the domain of coordinates accessible to the drops -- including their physical position, velocity, size, and temperature -- into computational cells and keeping a value of f in each cell. The computational cells are fixed in time as in an Eulerian fluid dynamics calculation, and derivatives of f are approximated by taking finite differences of the cell values. This approach, which we call the full spray equation method, suffers from two principal drawbacks. First there are large numerical diffusion and dispersion errors (5) associated with convection through the fixed Eulerian mesh. Second, the computer storage requirements are enormous. For example, in two space dimensions, the distribution function f has at least six independent variables. Since at least ten divisions are required to resolve changes in each variable, at least 10^6 computational cells are required -- exceeding the storage limits of modern computers.

In a second approach to solving the spray equation, which has been used since the early sixties (6,7), the spray is discretized into computational particles that follow drop characteristic paths. Each particle represents a number of drops of identical size, velocity, and temperature. Actually, the early particle methods only calculated individual droplet trajectories, assuming the drops had no influence on the gas. A later method (8), which was restricted to steady state sprays, included the complete coupling between the drops and gas. This later method also discretized the assumed droplet probability distribution function at the upstream boundary, which is determined by the atomization process, by subdividing the domain of coordinates into computational cells. Then one parcel was injected for each cell.

In an important advance in numerical methods for sprays, Dukowicz (9) suggested that the ideas of the Monte Carlo method could be combined with particle methods for spray calculations. For example in the method of Dukowicz, which we call the stochastic particle method, the distribution of drops at the upstream boundary is sampled stochastically by a relatively small number of computational particles. The droplet distribution function is obtained by averaging over a long time in steady-state calculations, or over many calculations in unsteady problems. The stochastic particle method can calculate unsteady sprays, and it accounts for the full coupling due to mass, momentum, and energy exchanges between the drops and

framework within which to include some important new physical effects in spray calculations. In particular, using the stochastic particle method much progress has been made in discovering the mechanisms that determine spray droplet sizes.

The first major extension of the stochastic particle method was supplied by O'Rourke (10), who developed and applied a method for calculating droplet collisions and coalescences. Consistent with the stochastic particle method, collisions are calculated by a statistical, rather than a deterministic, approach. The probability distributions governing the number and nature of the collisions between two drops are sampled stochastically. The method was initially applied to the diesel sprays of Hiroyasu and Kadota (11), where it was found that coalescences caused a seven-fold increase in the mean drop size (10). Many subsequent studies (12-14) have corroborated the importance of drop collisions in diesel-type sprays.

A second major extension of the stochastic particle method was the recent addition by Reitz and Diwakar of a method for calculating droplet breakup (15,16). In comparisons of calculations and experiments, it was found that drop breakup was important in the hollow-cone and full-cone sprays typically used in direct-injected stratified charge engines. In fact, the drop sizes downstream of the injector were found to be determined primarily by a competition between coalescences and breakups. Reitz and Diwakar (16) also suggested a numerical method for calculating atomization that uses a droplet breakup model. Hereafter we shall for brevity use the name Reitz when referring to this work. In this method, one injects droplets whose diameter equals the nozzle exit diameter. The breakup of these large drops is then accomplished by the breakup model. This method for calculating atomization makes the reasonable assumption that the dynamics and breakup of a liquid jet column are indistinguishable from those of a train of drops with equal diameter. Although it requires further experimental validation, the method promises to remove one of the major weaknesses of current spray calculations -- the uncertainty in the specification of upstream boundary conditions.

The purpose of the present paper is to present an alternative model for droplet breakup and to independently corroborate the findings of Reitz and Diwakar concerning the importance of droplet breakup.

The model is based on an analogy, suggested by Taylor (17), between an oscillating and distorting droplet and a spring-mass system. The restoring force of the spring is analogous to the surface tension forces. The external force on the mass is analogous to the gas aerodynamic force. To the analogy we have added the damping forces due to liquid viscosity. We call this model the TAB (Taylor Analogy Breakup) model. The TAB model has several advantages over that of Reitz. One is that it predicts, as pointed out by Taylor (17), that there is not a unique critical Weber number for breakup; whether or not a droplet breaks up depends on the history of its velocity relative to the gas. The Weber number is a dimensionless measure of the relative importance of gas aerodynamic forces that distort a drop and surface tension forces that restore sphericity. Second, the effects of liquid viscosity are included. Although these effects are negligible for large drops, liquid viscosity can significantly affect the oscillations of small drops. Third, the model predicts the state of oscillation and distortion of droplets. Thus, if information is available on how distortions and oscillations affect the exchange rates of mass, momentum, and energy between the droplets and gas, this information can be incorporated in the model. Fourth, the model gives drop sizes that are more consistent with experimentally-determined mechanisms of liquid jet breakup (18,19). There is a further advantage if our droplet breakup model is used as a means to calculate liquid jet breakup. This is that the model predicts a velocity of the product drops normal to the path of the original parent droplet. This normal velocity determines an initial spray angle that is in good agreement with measured spray angles (18). Thus, there is no need to input the spray angle.

The major limitation of the TAB model is that we can only keep track of one oscillation mode, and in reality there are many such modes. Thus, more accurately, the Taylor analogy should be between an oscillating droplet and a sequence of spring-mass systems, one for each mode of oscillation. We keep track only of the fundamental mode corresponding to the lowest order spherical zonal harmonic (20) whose axis is aligned with the relative velocity vector between droplet and gas. This is the longest-lived and, therefore, the most important mode of oscillation, but for large Weber numbers other modes are certainly excited and contribute to drop breakup. Despite this limitation, we get good agreement between our theory and experimentally observed breakup times.

In the following section we give the equations used by the TAB method. These equations contain four dimensionless constants that are determined by some theoretical and experimental results. It is next shown how the model predicts and continuously connects breakup times experimentally observed for the "bag" and "stripping" breakup regimes. The bag mode occurs when the Weber number is slightly larger than a critical value, and the stripping mode occurs for Weber numbers much larger than this same critical value.

We next show how the TAB model predicts the velocity of the product drops normal to that of the parent drop and how this normal velocity is consistent with some measured spray angles (18). Thus, the spray angle is automatically calculated by the TAB method. In contrast, in the method of Reitz (16) the spray angle must be independently specified when one injects particles into the computational domain.

The Taylor analogy equations do not predict product drop sizes, and we next give the product drop size equation that we use and motivate this equation by an energy conservation argument. It is shown that for large Weber numbers, the product drop sizes are determined by a Weber number criterion.

The numerical implementation of the model is next described. Finally, we present computa-

tional results and compare these with the experiments of Hiroyasu and Kadota (11) and the calculations of Reitz (16). The two models give different drop sizes near the injector because they use different breakup times. Downstream the models give similar results when the back-pressure is lowest, but at higher back-pressures the TAB method gives larger drop sizes than Reitz's calculations and the experiments. We give some possible reasons for the discrepancy.

THE TAB MODEL EQUATIONS

We now give the equations of the model and tell how some of the dimensionless constants are determined. The equation of a damped, forced harmonic oscillator is

$$m\ddot{x} = F - kx - d\dot{x} , \tag{1}$$

where we take x to be the displacement of the equator of the droplet from its equilibrium position. In accordance with the Taylor analogy, the physical dependencies of the coefficients in Eq. (1) are

$$\frac{F}{m} = C_F \frac{\rho_g u^2}{\rho_\ell r} ,$$

$$\frac{k}{m} = C_k \frac{\sigma}{\rho_\ell r^3} , \tag{2}$$

and

$$\frac{d}{m} = C_d \frac{\mu_\ell}{\rho_\ell r^2} ,$$

where ρ_g and ρ_ℓ are the gas and liquid densities, u is the relative velocity between the gas and droplet, r is the droplet radius, σ is the gas-liquid surface tension coefficient, and μ_ℓ is the liquid viscosity. Values for the dimensionless constants C_F, C_k, and C_d will be given shortly. We assume that drop breakup occurs if and only if $x > C_b r$, where C_b is an additional dimensionless constant.

Before solving Eq. (1), we nondimensionalize x by $C_b r$. Letting $y = x/(C_b r)$ and using Eq. (2) in Eq. (1) gives

$$\ddot{y} = \frac{C_F}{C_b} \frac{\rho_g}{\rho_\ell} \frac{u^2}{r^2} - \frac{C_k \sigma}{\rho_\ell r^3} y - \frac{C_d \mu_\ell}{\rho_\ell r^2} \dot{y} , \tag{3}$$

with breakup occurring if and only if $y > 1$. This is the equation we use in our breakup model. For constant relative speed u, the solution to Eq. (3) is

$$y(t) = \frac{C_F}{C_k C_b} We + e^{-C_d t_d} \left(y_0 - \frac{C_F}{C_k C_b} We \right) \cos \omega t$$

$$+ \frac{1}{\omega} \left(\dot{y}_0 + \frac{y_0 - \frac{C_F}{C_k C_b} We}{t_d} \right) \sin \omega t \Bigg| \tag{4}$$

where

$$We = \frac{\rho_g u^2 r}{\sigma} ,$$

$$y_0 = y(0) ,$$

$$\dot{y}_0 = \frac{dy}{dt}(0) ,$$

$$\frac{1}{t_d} = \frac{C_d}{2} \frac{\mu_\ell}{\rho_\ell r^2} ,$$

and

$$\omega^2 = C_k \frac{\sigma}{\rho_\ell r^3} - \frac{1}{t_d^2}$$

The overdamped case, $\omega^2 < 0$, occurs only for very small drops. The quantity We is the Weber number.

The dimensionless constants C_F, C_k, and C_d are determined by comparing with one experimental and two theoretical results. In shock experiments (21) the critical Weber number for breakup has been found to be $We_{crit} \approx 6$. In these experiments $t_d \approx \infty$ and $y_0 = \dot{y}_0 = 0$. Thus from Eq. (4),

$$y(t) = \frac{C_F}{C_k C_b} We (1 - \cos \omega t) \tag{5}$$

The model predicts breakup if and only if $y > 1$, which occurs if and only if

$$2 \frac{C_F}{C_k C_b} We > 1$$

Thus the model gives the experimental result if

$$\frac{C_k C_b}{C_F} = 2 We_{crit} = 12 \tag{6}$$

The constant C_k is obtained by matching to the fundamental oscillation frequency. Lamb (op. cit., p. 475) gives

$$C_k = 8 \tag{7}$$

For oscillations of the fundamental mode, Lamb (op. cit., p. 640) has derived

$$C_d = 5 , \tag{8}$$

mented mode the equator oscillates with exactly half the amplitude of the north and south poles (20). We postulate that breakup occurs if and only if the amplitude of oscillation of the north and south poles equals the drop radius. This criterion gives

$$C_b = \frac{1}{2} , \tag{9}$$

and, in conjunction with Eqs. (6) and (7),

$$C_F = \frac{1}{3} \tag{10}$$

COMPARISONS WITH EXPERIMENTAL BREAKUP TIMES

We will now show that the model predicts, and continuously connects, experimental breakup times in the stripping and bag breakup regimes. In shock experiments (21), it has been found that for large We the breakup times are proportional to

$$\sqrt{\frac{\rho_\ell}{\rho_g}}\,\frac{r}{u}$$

The breakup times that the model predicts for these experiments are obtained from Eq. (5). When We >> 1, the drop will break up after a small fraction of its oscillation period; that is, $\omega t_{bu} << 1$, where t_{bu} is the breakup time. In this limit

$$\cos \omega t_{bu} \approx 1 - \frac{\omega^2 t_{bu}^2}{2} ,$$

which when substituted into the right-hand side of Eq. (5) yields

$$1 - \frac{C_F}{C_b C_k} We \frac{\omega^2 t_{bu}^2}{2} \tag{11}$$

when y = 1. Neglecting liquid viscosity,

$$\omega^2 = C_k \frac{\sigma}{\rho_\ell r^3}$$

Substituting for ω^2 in Eq. (11) and solving for t_{bu} gives

$$t_{bu} = \sqrt{3}\sqrt{\frac{\rho_\ell}{\rho_g}}\,\frac{r}{u} \quad \text{(large We)} \tag{12a}$$

Ranger and Nicholls (22) give

$$t_{bu} = 8\sqrt{\frac{\rho_\ell}{\rho_g}}\,\frac{r}{u} ,$$

trace of mist," is defined with some uncertainty. Reitz (16) uses

$$t_{bu} = 20\sqrt{\frac{\rho_\ell}{\rho_g}}\,\frac{r}{u} \tag{12b}$$

based on an extrapolation of initial mass loss rates in the experiments of Reinecke and Waldman (23). Thus there are big differences in the proportionality constants used for the large Weber number breakup time. As we shall see later the computational results are sensitive to the value of this proportionality constant. Further experiments and comparisons with experiments are needed to determine its value more precisely.

When We is close to its critical value (bag breakup regime) the breakup time is determined from Eq. (5) by $\omega t_{bu} = \pi$, or

$$t_{bu} = \pi\sqrt{\frac{\rho_\ell r^3}{8\sigma}} \quad (We = We_{crit}) \tag{13}$$

This is just the half-period of the fundamental mode of oscillation. Reitz (16) uses the full period:

$$t_{bu} = \pi\sqrt{\frac{\rho_\ell r^3}{2\sigma}}$$

PREDICTION OF NORMAL PRODUCT DROP VELOCITY AND SPRAY ANGLES

The TAB model also predicts a velocity of the product drops normal to the path of the parent drop. At the time of breakup, the equator of the drop is traveling outward with velocity $\dot{x} = C_b r\dot{y}$. It seems reasonable that the product drops will have normal velocity

$$V_\perp = C_v C_b r\dot{y} , \tag{14}$$

where C_v is approximately unity. If liquid jet breakup is calculated by injecting drops whose radius is the injector radius, then Eq. (14) gives a spray angle in close agreement with experimental results (18). To see this, we note that from Eq. (5)

$$\dot{y} = \frac{C_F}{C_k C_b} We\,\omega^2 t_{bu} \tag{15}$$

at the time of drop breakup when We is large. Substituting from Eq. (15) into Eq. (14) and using the breakup time Eq. (12) and Eq. (10), results in

$$\tan\frac{\theta}{2} = \frac{V_\perp}{u} = C_v\frac{\sqrt{3}}{3}\sqrt{\frac{\rho_g}{\rho_\ell}} , \tag{16}$$

where θ is the spray angle. The experimental result (18) is

$$\tan\frac{\theta}{2} = \frac{\sqrt{3}}{3}\,\frac{2u}{3 + \frac{L/d}{3\,6}}\,\sqrt{\frac{\rho_g}{\rho_\ell}} \qquad (17)$$

for hole nozzles with inlet length L and diameter d. Equations (16) and (17) agree when $C_t = 1$ and L/d = 11.8. Equation (16) does not, of course, predict the dependence of the spray angle on nozzle L/d. It will be shown in the computational results section that by giving an initial oscillation to the large injected drops, the initial spray angle can be varied, and the effects of nozzle geometry changes can be included in numerical calculations.

DROP SIZES AFTER BREAKUP

To predict the drop sizes after breakup, we use an equation motivated by an analysis based on energy conservation. The analysis is not exact but predicts quite plausible sizes in the limits of bag and stripping mode breakup. In this analysis we equate the energy of the parent drop before breakup to the combined energies of the product drops after breakup. Before breakup, the energy of the parent drop in its own frame of reference is the sum of its minimum surface energy ($4\pi r^2\sigma$) and the energy in oscillation and distortion E_{osc}. If all the latter contribution were in the fundamental mode, one can show that

$$E_{osc} = \frac{4\pi}{5}\,\rho_\ell r^3(\dot{x}^2 + \omega^2 x^2) = \frac{\pi}{5}\,\rho_\ell r^5(\dot{y}^2 + \omega^2 y^2) \qquad (18)$$

In reality there is energy in other modes and we take

$$E_{osc} = K\,\frac{\pi}{5}\,\rho_\ell r^5(\dot{y}^2 + \omega^2 y^2) \qquad (19)$$

where K is the ratio of the total energy in distortion and oscillation to the energy in the fundamental mode. Thus the energy of the parent drop before breakup is

$$E_{old} = 4\pi r^2\sigma + K\,\frac{\pi}{5}\,\rho_\ell r^5(\dot{y}^2 + \omega^2 y^2) \qquad (20)$$

After breakup we assume the product drops are not distorted or oscillating. Thus the energy after breakup is the sum of the minimum surface energies of the product drops and the kinetic energy the product drops have due to their motion normal to the path of the parent drop. The first contribution is $4\pi r^2\sigma\, r/r_{32}$, where r_{32} is the Sauter mean radius of the size distribution of the product drops. Using Eq. (14), the kinetic energy of the product drops (in the frame of reference of the parent drop), is $1/6\,\pi r^5\rho_\ell\dot{y}^2$, where we take $C_p = 1$. Hence the total energy after breakup is

$$E_{new} = 4\pi r^2\sigma\,\frac{r}{r_{32}} + \frac{\pi}{6}\,r^5\rho_\ell\dot{y}^2 \qquad (21)$$

After equating E_{old} and E_{new} and using $y = 1$ and $\omega^2 = 8\sigma/\rho_\ell r^3$, one obtains after some algebraic manipulation

$$\frac{r}{r_{32}} = 1 + \frac{8K}{20} + \frac{\rho_\ell r^3}{\sigma}\,\dot{y}^2\left(\frac{6K-5}{120}\right) \qquad (22)$$

The value of K must be determined by comparisons with experimentally measured drop sizes. In our calculations we have used K = 10/3 because this predicts a product droplet Sauter mean radius of 6 in shock experiments (see Eq. (23) below), and this is the critical Weber number in these experiments.

In the bag breakup regime $\dot{y} \approx 0$ at breakup, and Eq. (22) gives

$$\frac{r}{r_{32}} = 7/3 .$$

In a shock experiment with We very large, one can show Eq. (22) gives

$$\frac{r}{r_{32}} \approx \frac{We}{6}$$

or

$$\frac{\rho_g u^2 r_{32}}{\sigma} = 6 . \qquad (23)$$

Thus the Weber number based on the product drop Sauter mean radius is 6.

For the distribution of sizes of the product drops we have used the χ-squared distribution. The breakup process will result in a distribution of sizes because many modes will be excited by aerodynamic interaction with the gas. Each mode will produce drops of a different size. In addition, during the breakup process there will be collisions and coalescences of the product drops, resulting in collisional broadening of the size distribution. For lack of further evidence for the form of the product drop distribution, we have chosen a χ-squared distribution because this was measured at downstream locations in the experiments of Hiroyasu and Kadota (11).

Equation (23) is a purely aerodynamic criterion for the product drop sizes. In contrast, to determine r_{32} Reitz (16) uses

$$\frac{We}{\sqrt{Re}} = \frac{\rho_g u^2 r_{32}}{\sigma}\sqrt{\frac{\nu}{u r_{32}}} = \frac{1}{2} , \qquad (24)$$

which is postulated by Nicholls (21) to determine the boundary between the bag and stripping breakup modes. The quantity ν is the kinematic viscosity of the gas. In introducing the drop Reynolds number Re Eq. (24) implies that at large We, viscous stripping of droplets from the parent drop is a dominant mechanism for parent drop breakup. This is inconsistent with experimental

depend on Re. It is also inconsistent with experimentally measured spray angles (18) and intact core lengths (19), which indicate a dominantly aerodynamic mechanism of liquid jet breakup.

NUMERICAL IMPLEMENTATION

In this section we describe the numerical implementation of the TAB method in the KIVA computer program (24). KIVA is a computer code for calculating two- and three-dimensional fluid flows with chemical reactions and fuel sprays. Sprays are calculated using the stochastic particle method. In addition to arrays specifying the particle position, velocity, size, and temperature, to implement the TAB method we keep two additional arrays specifying the values of y and $\dot{y}$ of each particle. Equation (4) is used to update the values of y and $\dot{y}$ each computational cycle as is described below.

For each particle we first calculate We, t_d, and ω^2. A value of $\omega^2 \le 0$ occurs only for very small drops for which distortions and oscillations are negligible. Thus if $\omega^2 \le 0$, we set $y^{n+1} = \dot{y}^{n+1} = 0$, where the superscript $n+1$ denotes the advanced-time value. If $\omega^2 > 0$, we next calculate the amplitude A of the undamped oscillation:

$$A^2 = \left(y^n - \frac{We}{12}\right)^2 + \left(\frac{\dot{y}^n}{\omega}\right)^2$$

If $We/12 + A \le 1.0$, then according to Eq. (4) the value of y will never exceed unity and breakup will not occur. Most particles will pass the test $We/12 + A \le 1.0$, and for these we simply update y and $\dot{y}$ using Eq. (4):

$$y^{n+1} = \frac{We}{12} + e^{-\frac{\Delta t}{t_d}}\left\{\left(y^n - \frac{We}{12}\right)\cos\omega\Delta t + \frac{1}{\omega}\left(\dot{y}^n + \frac{y^n - \frac{We}{12}}{t_d}\right)\sin\omega\Delta t\right\} \qquad (25a)$$

and

$$\dot{y}^{n+1} = \frac{\left(\frac{We}{12} - y^{n+1}\right)}{t_d} + e^{-\frac{\Delta t}{t_d}}\left\{\frac{1}{\omega}\left(\dot{y}^n + \frac{y^n - \frac{We}{12}}{t_d}\right)\cos\omega\Delta t - \left(y^n - \frac{We}{12}\right)\sin\omega\Delta t\right\} \qquad (25b)$$

These formulas assume that the coefficients of Eq. (3) are constant for the duration of time-step Δt. This is only approximately true, but relaxation [illegible] would necessitate a more costly direct numerical integration of Eq. (3).

If $We/12 + A \ge 1.0$, then breakup is possible. We then calculate the breakup time t_{bu} assuming that the drop oscillation is undamped for its first period. Again this will be true for all except very small drops. The time t_{bu} is the smallest root greater than t^n of the equation

$$\frac{We}{12} + A\cos\left[\omega(t - t^n) + \phi\right] = 1 \qquad (26)$$

where

$$\cos\phi = \frac{y^n - \frac{We}{12}}{A}$$

and

$$\sin\phi = -\frac{\dot{y}^n}{(A\omega)}.$$

If time $t^{n+1} = t^n + \Delta t$ is less than t_{bu}, then no breakup occurs this time-step, and we use Eq. (25) to update y and $\dot{y}$.

Breakup is calculated only if $t^n \le t_{bu} \le t^{n+1}$. In case of breakup, the breakup size r_{32} and normal velocity $V_\perp$ are evaluated using Eq. (22) and Eq. (14) with $\dot{y}$ evaluated at t_{bu}. The radius of the product drops is chosen randomly from a χ-square distribution with Sauter mean radius r_{32}. To conserve mass, the number of drops N associated with the computational particle is adjusted according to

$$N^{n+1} = N^n\left(\frac{r^n}{r^{n+1}}\right)^3$$

We also add to the particle velocity a component with magnitude $V_\perp$ normal to its relative velocity vector to the gas. The direction of this added component is randomly chosen in a plane normal to the relative velocity vector. This procedure does not conserve momentum in detail but it does so on the average. Following breakup, we assume the product drops are not distorted or oscillating, and accordingly we set $y^{n+1} = \dot{y}^{n+1} = 0$.

COMPUTATIONAL RESULTS

The experimental results of Hiroyasu and Kadota (11) have often been used (9,10,16) to validate numerical spray models because drop sizes were measured, albeit at only one axial location. In the experiment, an axisymmetric solid-cone diesel spray was injected into a chamber in which the back pressure was varied but the temperature was maintained at 293 K. Spray angle and tip penetration were measured from photographs of the backlighted spray. The drops were collected downstream in an emulsion that preserved their size. Average sizes and size distributions were reported for back pressures of 1.1, 3.0, and 5.0 MPa.

were performed with the mesh shown in Fig. 1. The computational region was 15 cm in the axial direction, which was resolved with 40 cells, and 3 cm in the radial direction, which was resolved with 25 cells. The cell dimensions were expanded with both axial and radial distance from the injector, where the smallest cells had radial cell size δr = 0.05 cm and axial cell size δz = 0.20 cm. The left boundary was a symmetry axis, the bottom boundary was a rigid free-slip wall, and the right and top boundaries were open constant pressure boundaries that allowed the flow to either enter or exit the mesh.

The Reitz method (16) was used to calculate atomization. Thus drops were injected with radius 0.015 cm, equal to the nozzle exit radius. These were injected at the lower left corner of the mesh in the axial direction. The velocity of the injected drops was calculated assuming a nozzle discharge coefficient of 0.705. In baseline calculations we injected 1.7×10^5 computational particles each second of problem time. This gave between 500 and 3000 particles in the computational mesh at steady-state conditions, the number varying with variation of the back-pressure. The results reported below did not change appreciably when this particle injection rate was varied.

With the exception of the breakup model, the same version of the KIVA program was used as in the study of Reitz (16). In particular, drop collisions and coalescences were calculated (10), and the drop-turbulence interaction effects were included (16).

Figure 2 shows the computed and experimentally measured spray tip penetrations. The computed tip was defined as that axial location below which 99% of the spray mass resided. Good agreement was obtained, with differences between experiment and calculation being comparable to the differences obtained on successive calculations using different particle injection rates. Reitz (16) obtained similar agreement. Spray tip penetration is fairly insensitive to many important physical parameters (10,16), and therefore this agreement, while gratifying, is not sufficient for model validation.

Spray angle is another global parameter that is not very sensitive to physical parameter variations. Figure 3 gives the computed and measured spray angles and shows typical spray particle plots at steady-state conditions. The calculated angle was defined as the smallest apex angle of a cone that contained 99% of the spray mass and whose apex was located at the injector. Evidently this definition gives a much wider cone than that measured from backlighted photographs. That the experimental comparison is not that bad, can be seen by the fact that for each back-pressure the ratio of the calculated to experimentally-measured spray angle is nearly 1.7

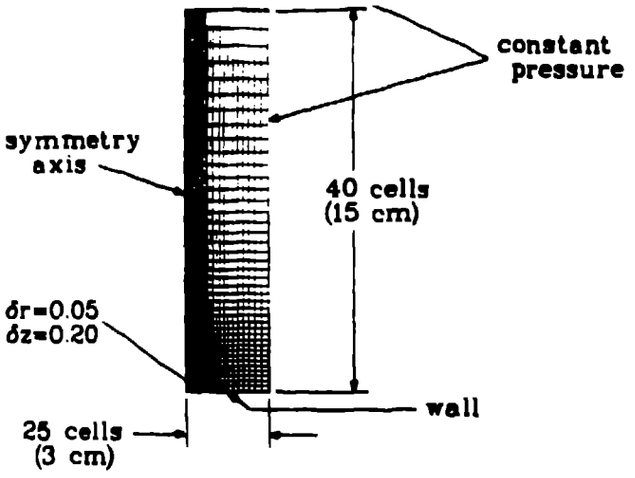

Fig. 1. Computational mesh for the numerical calculations of the Hiroyasu sprays.

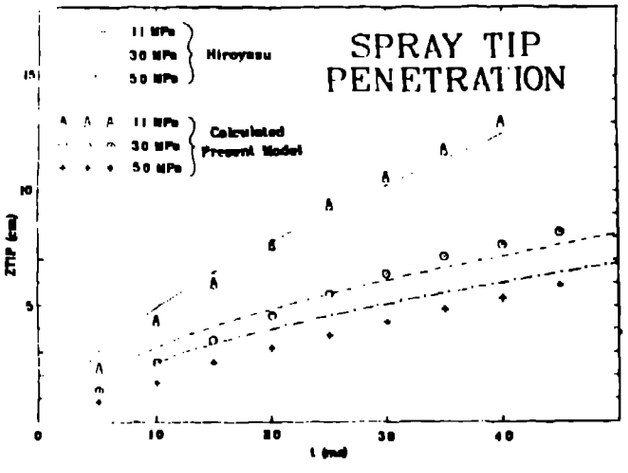

Fig. 2. Computed and measured spray tip penetrations.

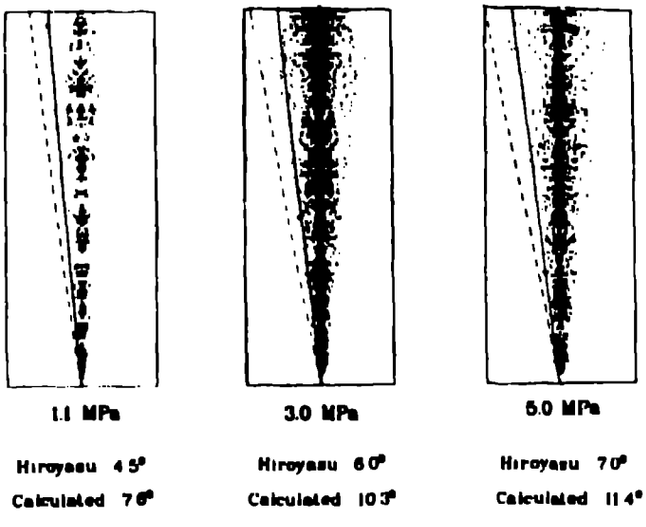

Fig. 3. Computed and measured spray angles and spray particle position plots.

mean radius versus axial distance from the injector, for the calculations of this paper and of Reitz (16). Also shown on each plot is the one reported data point of Hiroyasu and Kadota (11). Generally the curves can be broken into two sections. Close to the injector the drop sizes diminish rapidly as the large injected drops break up. Further downstream the drop sizes increase gradually because of drop coalescence. The most obvious difference between the calculations occurs near the injector, where the calculations of Reitz (16) have much larger drop sizes. This is due to the longer breakup time used in the study of Reitz [cf. Eq. (12)], which delays the breakup of the large injected drops.

Downstream the calculations give similar results when the back-pressure is 1.1 MPa. At higher back pressures, the TAB method gives larger drop sizes than Reitz's calculations between 20 and 80 mm from the injector, and both methods give larger drop sizes than the experiments 65 mm from the injector. The differences between the computed sizes of Reitz and of the TAB method are not surprising, considering the different formulas used to calculate the sizes of breakup product drops [cf. Eqs. (22) and (24)]. Better agreement between the TAB method results and experiments could be obtained by reducing either the breakup times or the sizes of breakup product drops. Since the breakup time we use is already small compared to that recommended by others [cf. Eqs. (12a) and (12b)], it seems most likely that drop sizes should be reduced by increasing the value of K in Eq. (22). This will be explored in future calculations.

Figure 7 shows drop sizes with and without drop breakup for the experiment with back-pressure 1.1 MPa. In these calculations we injected drops with an initial Sauter mean radius of 3 μm, as in the study of O'Rourke (10). With breakup, drop sizes are reduced by approximately 40%. Comparison of the breakup curve of Fig. 7 with the curves of Fig. 4 shows that nearly the same drop sizes are obtained downstream even though different size drops are injected. In Fig. 4,

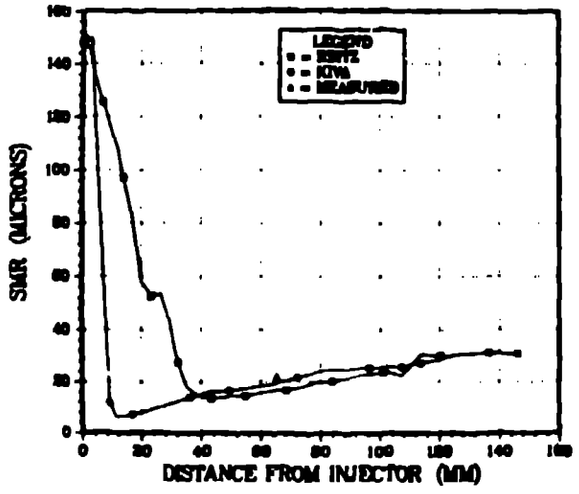

Fig. 4. Sauter mean radius versus distance from the injector for the 1.1 MPa case.

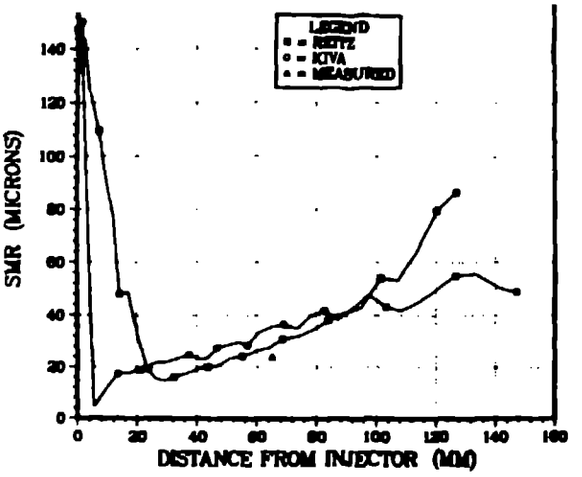

Fig. 5. Sauter mean radius versus distance from the injector for the 3.0 MPa case.

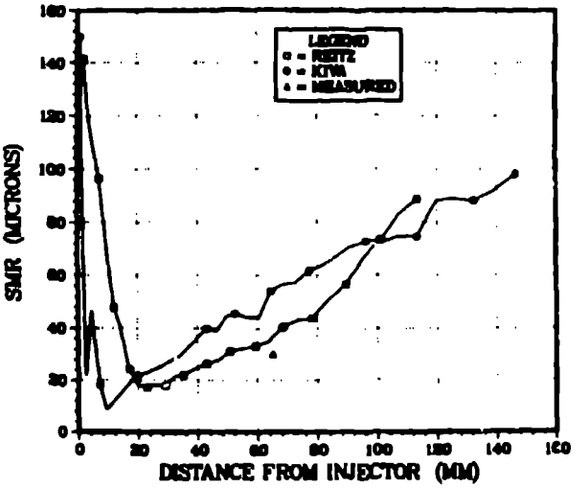

Fig. 6. Sauter mean radius versus distance from the injector for the 5.0 MPa case

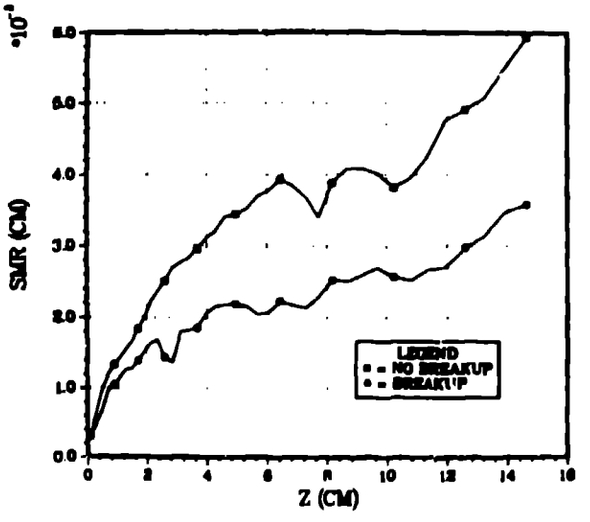

Fig. 7. Computed Sauter mean radii in calculations with and without breakup.

nozzle exit diameter. Thus drop breakup is probably significantly reducing downstream drop sizes in the calculations of Fig. 4.

Finally we perform a calculation to see if by injecting drops with an initial oscillation, we could influence the spray angle. Shown in Fig. 8 are particle plots from otherwise identical calculations with and without an initial oscillation given to the injected drops. It can be seen that with an initial oscillation of dimensionless amplitude 50.0, the computational particles are more dispersed near the injector. In order to influence the initial spray angle, it was found that the dimensionless amplitude of the initial oscillation must be comparable to the Weber number based on the nozzle radius and injection velocity. Further calculations are needed to obtain the dependence of initial spray angle on initial oscillation amplitude.

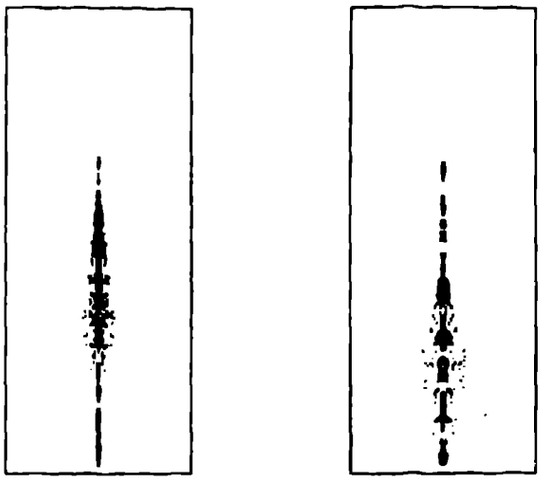

Fig. 8. Effect of an initial oscillation on the computed spray angle.

CONCLUSION

A numerical method, called the TAB (Taylor Analogy Breakup) method, has been developed for calculating droplet aerodynamic breakup in spray calculations using the stochastic particle method (9). The method has several significant advantages over previous methods for calculating drop breakup (15,16). Numerical calculations using the TAB method and the Reitz method (16) for calculating atomization, confirm the findings of Reitz (16) that drop breakup is important in the diesel sprays of Hiroyasu (11). Further experiments and experimental comparisons are needed to refine the TAB method and its dimensionless constants.

ACKNOWLEDGMENT

This work was supported by the United States Department of Energy, Office of Energy Research, Energy Conversion and Utilization Technologies Program.

REFERENCES

1. F. A. Williams, Phys. Fluids 1, 541 (1958).

2. E. H. Kennard, Kinetic Theory of Gases, McGraw-Hill Book Company Inc. (New York, 1938).

3. H. C. Gupta and F. V. Bracco, AIAA Journal 16, 10, 1053 (1978).

4. L. C. Hasselman and C. K. Westbrook, "A Theoretical Model for Fuel Injection in Stratified Charge Engines," SAE Paper 780138 (1978).

5. P. J. Roache, "Computational Fluid Dynamics," Hermosa Publishers (Albuquerque, New Mexico, 1982).

6. G. L. Borman and J. H. Johnson, "Unsteady Vaporization Histories and Trajectories of Fuel Drops Injected in Swirling Air." SAE Paper 598C (1962).

7. S. Lambiris, L. P. Combes, and R. S. Levine, "Stable Combustion Processes in Liquid Propellant Rocket Engines," Fifth Colloquium of the Combustion and Propulsion Panel, AGARD, 1962.

8. C. T. Crowe, M. P. Sharma, and D. E. Stock, J. Fluids Engr., 325 (1977).

9. J. K. Dukowicz, J. Comput. Phys. 35, 2, 229 (1980).

10. P. J. O'Rourke, "Collective Drop Effects on Vaporizing Liquid Sprays," Los Alamos National Laboratory report LA-9069-T (1981).

11. H. Hiroyasu and T. Kadota, "Fuel Droplet Size Distribution in Diesel Combustion Chamber," SAE F per 740715 (1974).

12. L. Martinelli, R. D. Reitz, and F. V. Bracco, "Comparison of Computed and Measured Dense Spray Jets," Ninth International Colloquium on Dynamics of Explosions and Reactive Systems, Poitiers, France, 1983.

13. A. U. Chatwani and F. V. Bracco, "Computation of Dense Spray Jets," ICLASS-85, London, 1985.

14. F. V. Bracco, "Modeling of Engine Sprays," SAE Paper 850394 (1985).

15. R. D. Reitz and R. Diwakar, "Effect of Drop Breakup on Fuel Spays," SAE paper 860469 (1986).

16. R. D. Reitz and R. Diwakar, "Structure of High-Pressure Fuel Sprays," SAE Paper 870598 (1987).

Drop in a High Speed Air Stream," The Scientific Papers of G. I. Taylor, ed. G. K. Batchelor, Vol. III, University Press, Cambridge, 1963.

18. R. D. Reitz and F. V. Bracco, "On the Dependence of Spray Angle and Other Spray Parameters on Nozzle Design and Operating Conditions," SAE Paper 790494 (1979).

19. B. Chehroudi, S. H. Chen, F. V. Bracco, and Y. Onuma, "On the Intact Core of Full-Cone Sprays," SAE Paper 850126 (1985).

20. H. Lamb, Hydrodynamics, Dover Publications (New York, 1932).

21. J. A. Nicholls, "Stream and Droplet Breakup by Shock Waves," NASA-SP-194, Eds. D. T. Harrje and F. H. Reardon, 1972, p. 126-128.

22. A. A. Ranger and J. A. Nicholls, AIAA Journal 7, 2, 28 (1969).

23. W. G. Reinecke and G. D. Waldman, "A Study of Drop Breakup Behind Strong Shocks with Applications to Flight," AVCO Report AVSD-0110-70-RR, May 1970.

24. A. A. Amsden, et al., "Improvements and Extensions to the KIVA Computer Program," Los Alamos National Laboratory report LA-10534-MS (October 1985); A. A. Amsden, et al., "KIVA: A Computer Program for Two- and Three-Dimensional Fluid Flows with Chemical Reactions and Fuel Sprays," Los Alamos National Laboratory report LA-10245-MS (February 1985).